

# Electronic and optical properties of Cr and Cr-N doped anatase TiO<sub>2</sub> from screened Coulomb hybrid calculations

Veysel Çelik and Ersen Mete\*

Department of Physics, Balıkesir University, Balıkesir 10145, Turkey

(Dated: March 20, 2013)

We studied the electronic and atomic structures of anatase TiO<sub>2</sub> codoped with Cr and N using hybrid density functional theory calculations. Nonlocal screened Hartree-Fock exchange energy is partially mixed with traditional semilocal exchange part. This not only heals the band gap underestimation but also improves the description of anion/cation-driven impurity states and magnetization of the dopants. Cr and/or N doping modifies the valence and conduction band edges of TiO<sub>2</sub> leading to significant band gap reduction. Hence, Cr, N and Cr-N doped TiO<sub>2</sub> are promising for enhanced photoactivity.

PACS numbers: 71.20.Nr, 71.55.-i, 61.72.Bb

## I. INTRODUCTION

For photocatalysis, titanium dioxide (TiO<sub>2</sub>) offers excellent oxidation and charge transport properties together with its wide availability, nontoxicity, and chemical stability. For this reason, it finds many useful applications such as photogeneration of hydrogen from water, degradation of pollutants under visible light irradiation and production of hydrocarbon fuels and dye sensitized solar cells (DSSC).[1–4] Among the other polymorphs the anatase phase exhibits higher catalytic activity.[5]

One important limitation is that anatase TiO<sub>2</sub> has a wide band gap of  $\sim 3.2$  eV [6] and can only absorb in the ultraviolet (UV) region ( $\lambda < 380$  nm). This seriously reduces solar energy utilization to  $\sim 5\%$ . Substitutional cation and/or anion modified titania has been proposed as an effective approach to get catalytic activity under visible light irradiation.[7–13] Recent experiments have shown that Cr-N codoping in TiO<sub>2</sub> drastically enhances absorbance.[14, 15] Moreover, Cr and Cr-N dopings were reported to increase the visible light reactivity with increasing Cr incorporation. [16, 17] Ferromagnetism has also been observed in Cr doped anatase films.[18, 19] Theoretical studies predicted magnetization per Cr much larger than experimental findings.[20, 21] Pure density functional theory (DFT) methods unreliably estimate half-metallic character for Cr doped TiO<sub>2</sub>[21, 22]. For the optical properties, hybrid theoretical approaches has been recently used to get improved quantitative agreement with the experimental data.[15, 23] Detailed electronic structure investigations are still needed to get a proper description of band gap features for the doped systems.

In this present work, we used screened Coulomb potential hybrid DFT calculations to investigate the modifications of the band gap properties of TiO<sub>2</sub> induced by Cr and Cr-N dopants and their effect on the correspond-

ing absorption spectra. Formation energies have been calculated as a function of oxygen chemical potential to compare thermodynamical stability of the doped structures. We also obtained the magnetic moments and the charge states of Cr and N species.

## II. THEORETICAL METHOD

For all systems, our calculations were performed based on the spin polarized hybrid density functional theory as implemented in the Vienna *ab-initio* simulation package (VASP).[25] Ionic cores and valence electrons were treated by projector-augmented waves (PAW) method.[26, 27] The kinetic energy cutoff value was determined to be 400 eV.

Pure DFT describes impurity and defect associated properties of transition metal oxides incorrectly. For example, TiO<sub>2</sub> is predicted to be metallic in oxygen vacancy cases.[28] However, experimental studies show a semiconducting nature. This failure of DFT lies in the approximations to the exchange-correlation (XC) energy being usually local or semilocal. This flaw can be patched by using hybrid methods where a portion of the non-local exact exchange is admixed with the traditional semilocal exchange. We used the Heyd-Scuseria-Ernzerhof hybrid XC functional (HSE06) [29–31] based on screened Coulomb potential reducing the self-interaction error. Technically, this results in a rapid spatial decay of HF exchange which improves the convergence behavior of self-consistent iterations. The HSE exchange is derived from the PBE0[32, 33] exchange by range separation and then by cancellation of counteracting long range HF and PBE contributions, as,

$$E_x^{\text{HSE}} = aE_x^{\text{HF,SR}}(\omega) + (1-a)E_x^{\text{PBE,SR}}(\omega) + E_x^{\text{PBE,LR}}(\omega),$$

where  $\omega$  is the range separation parameter for the screening and  $a$  is the mixing coefficient. The parameter of  $\omega = 0.2 \text{ \AA}^{-1}$  is used for the exchange contributions as suggested for the HSE06 functional.[34] We determined the mixing ratio of the exact exchange to be 22% so that

---

\*Corresponding author: e-mail: emete@balikesir.edu.tr

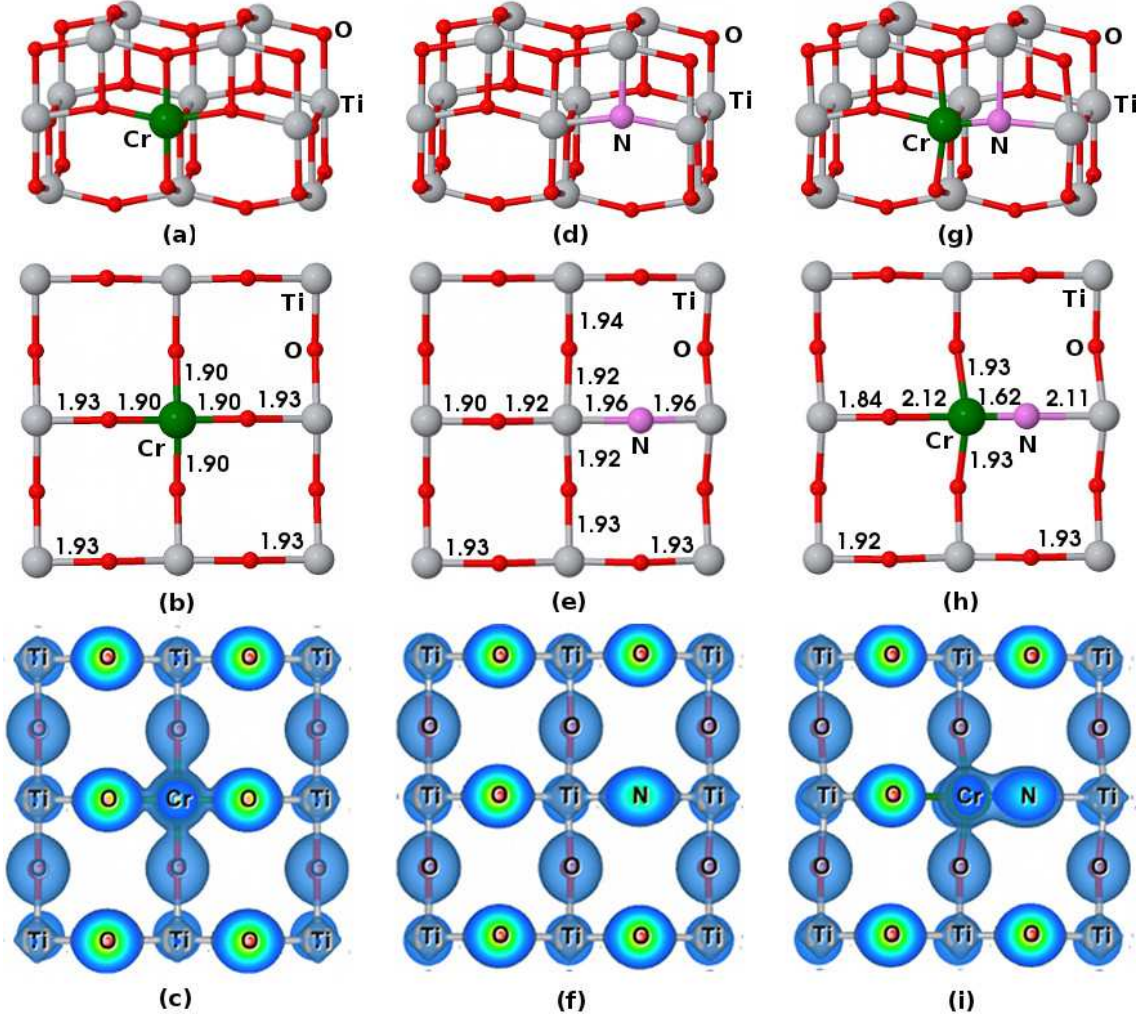


FIG. 1: Relaxed geometries and total charge densities of substitutional N (a-c), Cr (d-f) and Cr-N (g-i) in anatase  $\text{TiO}_2$ .

calculated band gaps and lattice constants for both the anatase and the rutile polymorphs show good agreement with the experimental values.[13]

In order to model the doped systems we constructed a 108-atom supercell by  $3 \times 3 \times 1$  replication of the conventional anatase unit cell. This structure is sufficiently large to accommodate spatial separation between the periodic images of the defects. We traced all possible Cr and N doping configurations. In particular, For Cr/N codoping, the structure shown in Fig. 1 is found to be energetically the most favorable. For geometry optimization and density of states (DOS) calculations we used 8 special  $k$ -points to perform the Brillouin zone integrations. The calculated properties are converged such that they unnoticeably change when a higher  $k$ -point sampling is used. We required a precision of 0.015 eV/Å in the residual forces in every spatial component on all the atoms without fixing them to their bulk positions.

The formation energies of the defects were calculated

by using the formula,

$$E_f = E_{\text{doped}} - E_{\text{pure}} - n\mu_{\text{Cr}} - m\mu_{\text{N}} + n\mu_{\text{Ti}} + m\mu_{\text{O}},$$

where  $E_{\text{doped}}$  ( $E_{\text{pure}}$ ) is the total energy of doped (pure) supercell. The chemical potentials of Cr, N, Ti and O are denoted by  $\mu_{\text{Cr}}$ ,  $\mu_{\text{N}}$ ,  $\mu_{\text{Ti}}$  and  $\mu_{\text{O}}$ , respectively. Depending on the presence of Cr (N) substitutional dopant, the number  $n$  ( $m$ ) assumes values 0 or 1. In thermodynamical equilibrium, the chemical potentials of Ti and O varies depending on the growth environment and must also satisfy the restriction  $\mu_{\text{TiO}_2} = \mu_{\text{Ti}} + 2\mu_{\text{O}}$ . Under O-rich conditions,  $\mu_{\text{O}}$  is taken from molecular oxygen, and then  $\mu_{\text{Ti}} = \mu_{\text{TiO}_2} - E_{\text{O}_2}$ . Under Ti-rich conditions,  $\mu_{\text{Ti}}$  is derived from bulk (hcp) Ti ( $\mu_{\text{Ti}}^{\text{bulk}}$ ) and  $\mu_{\text{O}}$  is calculated from  $\mu_{\text{O}} = \frac{1}{2}(\mu_{\text{TiO}_2} - \mu_{\text{Ti}})$ . The remaining chemical potentials of Cr and N are taken from their natural phases ( $\mu_{\text{Cr}} = \frac{1}{2}(E_{\text{Cr}_2\text{O}_3} - \frac{3}{2}E_{\text{O}_2})$  and  $\mu_{\text{N}} = \frac{1}{2}E_{\text{N}_2}$ ).

Bader analysis quantitatively describes local charge depletion/accumulation. It involves integration of Bader volumes around atomic centers. These volumes are partitions of the real space delimited by local zero-flux sur-

TABLE I: Average charge states ( $e$ ) of dopants and their adjacent (nn) Ti and O atoms from Bader analysis.

Doping	Cr	N	Ti(nn)	O(nn)
none			+2.84	-1.43
N@O		-1.38	+2.31	
Cr@Ti	+2.30			-1.33
Cr/N	+2.29	-1.13	+2.81	-1.19

faces of charge density gradient vector field. We calculated charge states of atomic species (in Table I) using a grid based decomposition algorithm.[37]

### III. RESULTS & DISCUSSION

The bulk properties of pure anatase were calculated using the 108-atom supercell. Our HSE-predicted lattice parameters ( $a = 3.78$  Å,  $c = 9.45$  Å) and band gap value (3.23 eV in Fig. 2) show remarkable agreement with the experimental data. Since nitrogen doping case has been discussed in detail elsewhere,[13] we will focus on Cr and Cr-N doped anatase to elucidate the role of Cr in photoelectrochemistry of  $\text{TiO}_2$ .

**Cr-doped  $\text{TiO}_2$  :** Experiments report incorporation of chromium at substitutional sites forming single-crystalline Cr-doped  $\text{TiO}_2$ . [9, 15, 16, 18] They also conclude that if chromium oxide forms it must be highly dispersed and its size must be undetectably small. [14–18, 24] In order to model the structure we substituted one Cr atom at a Ti site in the anatase supercell forming sixfold coordination with the nearest neighbor oxygens as shown in Fig. 1. All Cr-O bonds are 1.90 Å and slightly shortened relative to those of the undoped  $\text{TiO}_2$ . The disturbance of the substitutional Cr on the lattice is very small agreeing with the X-ray diffraction (XRD) patterns. [17, 24] Under O-rich conditions, the formation energy of Cr@Ti doping has been calculated to be 1.06 eV (in Fig. 3). These energetics are sensitive to the choice of the XC functional. For example, McDonnell *et al.* found a value of 0.36 eV with HSE06-PBEsol method. [15] Under Ti-rich conditions the formation energy gets as large as 10.21 eV. Therefore, synthesis of substitutional Cr under O-rich conditions must be much easier as pointed out by previous calculations. [23]

Substitutional Cr introduces  $3d$  states which are dominant above the top of the valence band (VB) as presented in the corresponding projected DOS (PDOS) of Fig. 2. For the minority spin component, fully occupied Cr  $3d$  states appear isolated 1.07 eV above the valence band maximum (VBM). Our calculations are interestingly in agreement with the X-ray Photoemission Spectra (XPS) of Osterwalder *et al.* [18] who reported the formation of defect states at 1.0 eV above the VBM giving an intensity roughly proportional to the Cr concentration.

HSE06 functional not only gives the relative positions of the defect states in the band gap but also better describes the character of these states. For instance, unlike the full-potential linearized augmented plane wave (FLAPW) calculations of Ye *et al.* [20] and LDA study of Peng *et al.*, our HSE06 results predict Cr doped anatase to be semiconducting, not half-metallic.

Chromium significantly modifies the conduction band minimum (CBM), too, by introducing empty Cr  $3d$  states at the bottom of the CB. Widely dispersing Cr-induced states effectively reduce the calculated band gap from 3.23 eV to a value of 2.16(2.14) eV for the spin up(down) component. This band gap narrowing agrees well with the decrease of the binding energy of Cr  $3d$  from 3.2 eV to 2.20 eV observed in the XPS spectra. [18] Depending of the choice of XC flavor, the band gap reduction was calculated by the previous theoretical studies to be 1.2 eV, [20] and 0.34 eV [15] with FLAPW and HSE06-PBEsol methods, respectively.

XPS core level and valence band data show that the majority of Cr is present in the 3+ charge state. [9, 15, 16, 18] In addition, the room temperature magnetization measurements reveal a ferromagnetic state for all Cr-doped anatase films, with a saturation magnetic moment of  $\sim 0.6 \mu_B$  per Cr atom. [18] Similarly, Zhang *et al.* reported  $\text{Cr}^{3+}$ -associated ferromagnetism which increases up to  $\sim 0.42 \mu_B/\text{Cr}$  by lowering of oxygen pressures. [19] Theoretical studies, on the other hand, predicted a charge state of 4+ with a magnetization of  $2 \mu_B$ . [20, 22, 23] The discrepancy has been attributed to the possible presence of oxygen vacancies which leave excess charge in the samples reducing the charge state from  $\text{Cr}^{4+}$  to  $\text{Cr}^{3+}$ . However, without such a compensation, our HSE-calculated charge state of +2.3 and total magnetic moment of 1.21  $\mu_B$  per Cr show a significant improvement over the existing theoretical estimations.

**Cr/N-codoped  $\text{TiO}_2$  :** Substitutional codoping of Cr and N in the anatase form has been confirmed by XRD measurements for various impurity concentrations. [14–17, 23] Initially, we considered all possible doping configurations. After the relaxation, the Cr-N pairing shown in Fig. 1(g-h) yields the lowest total energy. The lattice gets slightly disturbed because of the strong Cr-N interaction leading to a bond length of 1.62 Å which is considerably shorter than the Ti-N bonding. The total charge density plots in Fig. 1(g) and Fig. 1(f) clearly shows the covalent character of Cr-N coupling while Ti-N bonding is more polarized.

We calculated the formation energy for Cr/N codoping to be 4.43 eV under O-rich conditions. It rises up to 8.93 eV under O-poor growth environment as shown in Fig. 3. The experimental realization of Cr-N codoping is expected to be energetically viable under oxidizing atmosphere in agreement with previous studies. [15]

The presence of substitutional N in the codoped anatase phase reduces the calculated magnetic moment to 1.00  $\mu_B$  relative to the case of Cr monodoping. Be-



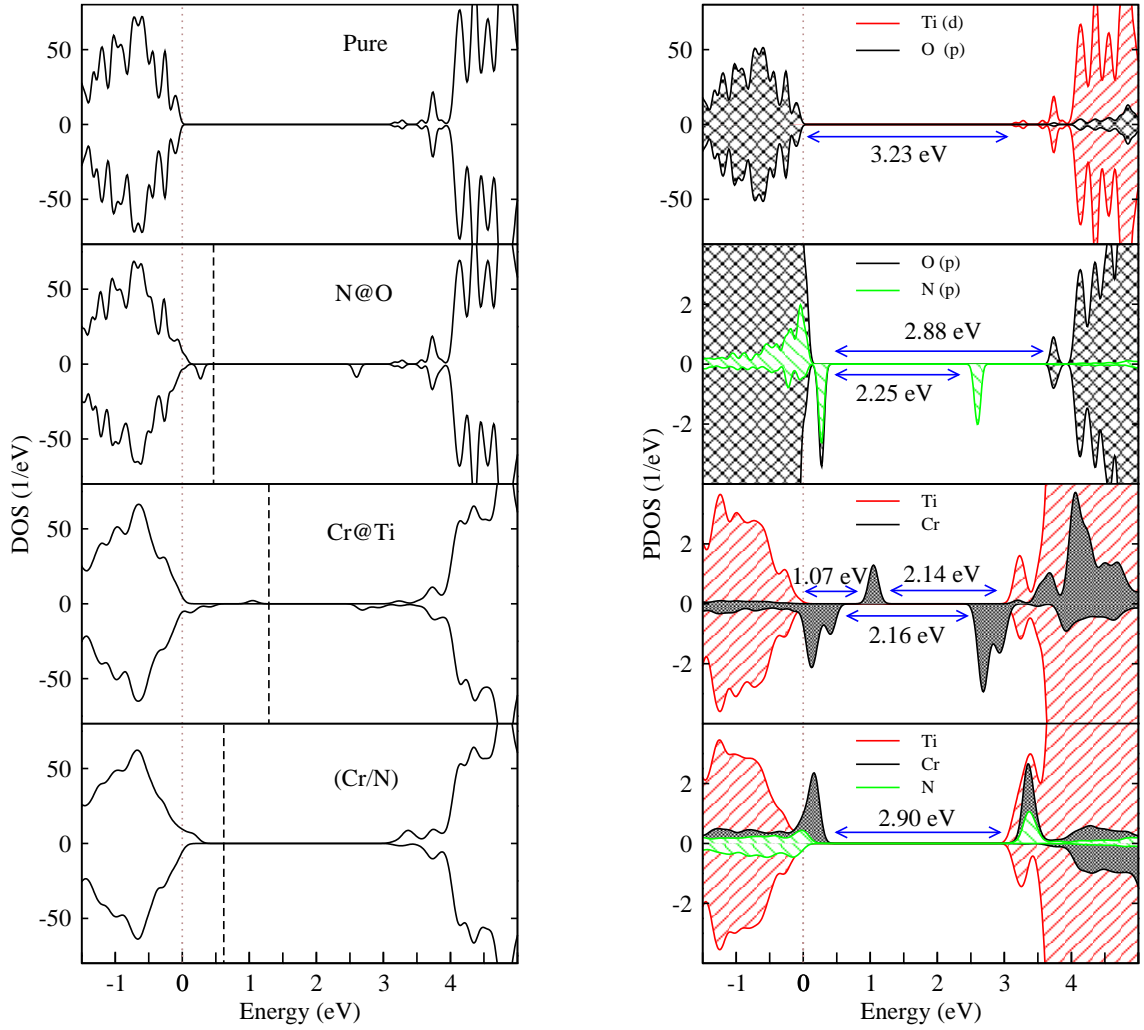


FIG. 2: Total (left) and projected (right) densities of states (DOS) of pure and doped (with Cr and/or N) anatase  $\text{TiO}_2$ , calculated with HSE06 functional. Dashed (dotted) line indicates the Fermi energy (the VBM of pure anatase).

sides, it insignificantly alters the charge state of Cr which is +2.29 as presented in Table. I. This indicates a strong delocalization of N  $2p$  states over  $\text{TiO}_2$  bands. The UV-vis reflectance spectral measurements of Li *et al.*[16] and the X-ray absorption spectroscopy (XAS) of Chiodi *et al.*[14] confirm the presence of  $\text{Cr}^{3+}$  species. Our HSE-calculated charge state is reasonably closer than the previous DFT+U predicted Mulliken charges on the substitutional Cr when N dopant is present.[23]

Strong Cr-N pair interaction exhibits interesting features in the electronic properties in Fig. 2. First, the isolated impurity states associated with Cr  $3d$  and N  $2p$  in the (Cr@Ti) and (N@O) monodoping cases mutually passivate each other giving a clean band gap. This eliminates the possibility of photo-generated charge recombination due to well localized trap states. Secondly, the Cr and N concentration of  $\sim 0.93\%$  in the computational cell causes a band gap reduction of 0.3 eV. McDonnell *et al.* calculated 2.66 eV band gap for Cr/N codoping by using HSE06-PBESol XC functional.[15] Chiodi *et al.*

reported the appearance of codoping-induced and Cr  $3d$  dominant states at the top of the VB which translates to a band gap of 2.8 eV.[14] This observation nicely fits in our PDOS structure in Fig. 2 with an estimated band gap of 2.9 eV. For higher dopant concentrations, experiments report increased gap narrowing causing significantly red-shifted optical absorption.[14–16] Thirdly, N  $2p$  states which appear in the monodoping case (N@O) in Fig. 2 significantly delocalize over the VB and the CB when Cr is present (Cr/N) due to strong Cr-N interaction. This PDOS feature shows remarkable agreement with the experimental observations.[14, 16] Therefore, N has a weaker effect on the optical response than Cr which dominantly modifies the band edges of  $\text{TiO}_2$ .

We calculated the absorption spectra of Cr- and Cr/N-doped cases in comparison with pure anatase (see Fig. 4). Cr seems to be absorbing in the visible region significantly better than the Cr-N codoping. However, PDOS structure of Cr@Ti shows that the overall photocatalytic efficiency might be lower than the Cr/N case due to

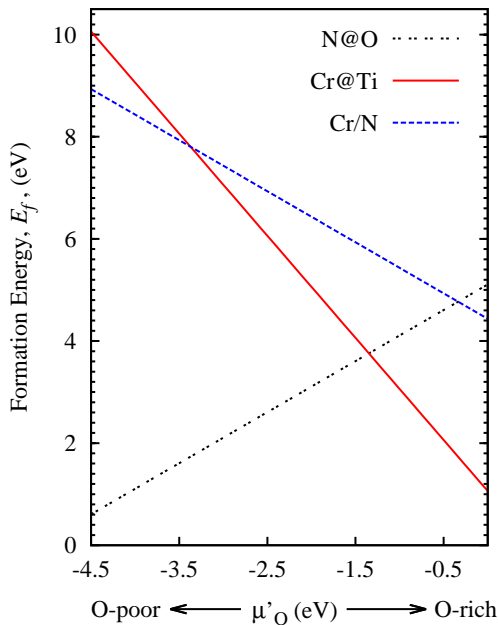


FIG. 3: Calculated formation energies as a function of the oxygen chemical potential (relative to the value at its molecular gas phase) for Cr, N mono- and Cr/N co-doped TiO<sub>2</sub> structures..

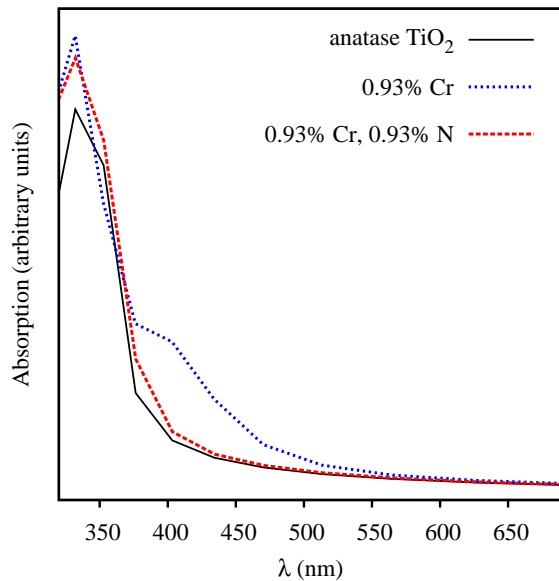


FIG. 4: Calculated absorption spectra for pure, Cr- and Cr/N-doped anatase TiO<sub>2</sub> structures.

the charge recombination in the presence of localized 3d gap states. In fact, Cr-N codoped TiO<sub>2</sub> exhibits relatively higher catalytic reactivity under visible light irradiation.[16]

#### IV. CONCLUSIONS

The electronic, magnetic and optical properties of Cr- and Cr/N-doped anatase TiO<sub>2</sub> have been investigated by means of screen Coulomb hybrid calculations. Hybrid functionals incorporating exact exchange terms not only improve the description of defect states but also are promising to predict magnetization properties of *d*-band dopants. We have shown the dominant character of Cr in modifying the band edges of anatase. Substitutional Cr with or without N is very effective in band gap reduction causing significant red-shift of the absorption edge into the visible spectral region. Isolated N 2*p* states get delocalized over TiO<sub>2</sub> bands due to mutual passivation by Cr 3*d* states giving a clean band gap for Cr/N-codoping. Thus, the enhancement of the optical absorption is emergent. Moreover, the calculations imply that the substitutional Cr and N pair reduces electron-hole recombination rate improving the overall photocatalytic performance.

#### Acknowledgments

This study was supported in part by TÜBİTAK, The Scientific and Technological Research Council of Turkey (Grant No. 110T394) through the computational resources provided by ULAKBİM, Turkish Academic Network & Information Center.

- 
- [1] A. Fujishima, K. Honda, Nature (London) **238**, 37 (1972).
  - [2] M. Grätzel, Nature (London) **414**, 338 (2001).
  - [3] S. U. M. Khan, M. Al-Shahry, W. B. Ingler, Jr., Science

- 297**, 2243 (2002).
- [4] O. K. Varghese, M. Paulose, T. J. LaTempa, C. A. Grimes, Nano Lett. **9**, 731 (2009).
- [5] M. Xu, Y. Gao, E. M. Moreno, M. Kunst, M. Muhler, Y.

- Wang, H. Idriss, C. Wöll, Phys. Rev. Lett. **106**, 138302 (2011).
- [6] H. Tang, H. Berger, P. E. Schmid, F. Levy, G. Burri, Solid State Commun. **87**, 847 (1993). Phys. Rev. B **18**, 5606 (1978).
- [7] P. Wang, Z. Liu, F. Lin, G. Zhou, J. Wu, W. Duan, B.-L. Gu, S. B. Zhang, Phys. Rev. B **82**, 193103 (2010).
- [8] H. Yu, H. Irie, and K. Hashimoto, J. Am. Chem. Soc. **132**, 6898 (2010).
- [9] W. Zhu, X. Qiu, V. Iancu, X.-Q. Chen, H. Pan, W. Wang, N. M. Dimitrijevic, T. Rajh, H. M. Meyer, M. P. Paranthaman, G. M. Stocks, H. H. Weitering, B. Gu, G. Eres, Z. Zhang, Phys. Rev. Lett. **103**, 226401 (2009).
- [10] R. Long, N. J. English, Phys. Rev. B **83**, 155209 (2011).
- [11] T. Yamamoto, T. Ohno, Phys. Rev. B **85**, 033104 (2012).
- [12] W.-J. Yin, S.-H. Wei, M. M. Al-Jassim, Y. Yan, Phys. Rev. Lett. **106**, 066801 (2011).
- [13] V. Çelik and E. Mete, Phys. Rev. B **86**, 205112 (2012).
- [14] M. Chiodi, C. Parks Cheney, P. Vilmercati, E. Cavaliere, N. Mannella, H. H. Weitering and L. Gavioli, J. Phys. Chem. C, **116**, 311-318, (2012).
- [15] K. A. McDonnell, N. J. English, M. Rahman and D. P. Dowling, Phys. Rev. B **86**, 115306, (2012).
- [16] Y. Li, W. Wanga, X. Qiu, L. Song, H. M. Meyer, M. P. Paranthaman, G. Eres, Z. Zhang, B. Gua, Appl. Catal., B:Environ. **110**, 148-153, (2011).
- [17] L. Liu, S. Chen, W. Sun and J. Xin, J. Mol. Struct. **1001**, 23-28, (2011).
- [18] J. Osterwalder, T. Droubay, T. Kaspar, J. Williams, C. M. Wang, S. A. Chambers, Thin Solid Films **484**, 289, (2005).
- [19] X. Zhang, W. Wang, L. Li, Y. Cheng, K. Luo, H. Liu, J. Phys. D:Apple. Phys. **41** 015005 (2008).
- [20] L.-H. Ye and A. J. Freeman, Phys. Rev. B **73**, 081304(R) (2006).
- [21] H. Peng, J. Li, S.-S. Li, J.-B. Xia, J. Phys.: Condens. Matter **20**, 125207 (2008).
- [22] C. Di Valentin, G. Pacchioni, A. Kudo, Chem. Phys. Lett. **469**, 166 (2009).
- [23] M. E. Kurtoglu, T. Longenbach, K. Sohlberg, and Y. Gogotsi, A.J. Phys. Chem. C, **115**, 17392-17399, (2011).
- [24] C.-C. Pan and J. C. S. Wu, Mat. Chem. and Phys. **100**, 102-107, (2006).
- [25] G. Kresse, J. Hafner, Phys. Rev. B, **47**, 558 (1993).
- [26] P. E. Blöchl, Phys. Rev. B **50**, 17953 (1994).
- [27] G. Kresse, J. Joubert, Phys. Rev. B **59**, 1758 (1999).
- [28] H. Unal, E. Mete, Ş. Ellialtıoğlu, Phys. Rev. B **84** 115407 (2011).
- [29] J. Heyd, G. E. Scuseria, M. Ernzerhof, J. Chem. Phys. **118**, 8207 (2003).
- [30] J. Heyd, G. E. Scuseria, M. Ernzerhof, J. Chem. Phys. **124**, 219906 (2006).
- [31] J. Paier, M. Marsman, K. Hummer, G. Kress, I. C. Gerber, J. G. Angyan, J. Chem. Phys. **125**, 249901 (2006).
- [32] J. P. Perdew, K. Burke, M. Ernzerhof, Phys. Rev. Lett. **77**, 3865 (1996), Phys. Rev. Lett. **78**, 1396 (1997).
- [33] C. Adamo, V. Barone, J. Chem. Phys. **110**, 6158 (1999).
- [34] A. V. Krukau, O. A. Vydrov, A. F. Izmaylov, G. E. Scuseria, J. Chem. Phys. **125**, 224106 (2006).
- [35] A. D. Becke, J. Chem. Phys. **98**, 1372 (1993); **99**, 5648 (1993).
- [36] J. P. Perdew, M. Ernzerhof, K. Burke, J. Chem. Phys. **105**, 9982 (1996).
- [37] W. Tang, E. Sanville, and G. Henkelman, J. Phys.: Condens. Matter **21**, 084204 (2009).
- [38] E. Mete, D. Uner, O. Gulseren, Ş. Ellialtıoğlu, Phys. Rev. B **79**, 125418 (2009).
- [39] J. K. Burdett, T. Hughbanks, G. J. Miller, J. W. Richardson, Jr., J. V. Smith, J. Am. Chem. Soc. **109**, 3639 (1987).